

Water vapor and silicon monoxide maser observations in the protoplanetary nebula OH 231.8+4.2

J.-F. Desmurs¹, J. Alcolea¹, V. Bujarrabal², C. Sánchez Contreras³, and F. Colomer²

¹ Observatorio Astronómico Nacional, C/Alfonso XII 3, E-28014 Madrid, Spain, e-mail: j.f.desmurs@oan.es

² Observatorio Astronómico Nacional, Apartado 112, Alcalá de Henares, E-28803 Madrid, Spain

³ Dpto. Astrofísica Molecular e Infrarroja (DAMIR), Instituto de Estructura de la Materia - CSIC, C/Serrano 121, E-28006 Madrid, Spain

Received: 12/12/2006; Accepted: 09/03/2007

ABSTRACT

Context. OH 231.8+4.2 is a well studied preplanetary nebula (pPN) around a binary stellar system that shows a remarkable bipolar outflow.

Aims. To study the structure and kinematics of the inner 10-80 AU nebular regions probed by SiO and H₂O maser emission, where the agents of wind collimation are expected to operate, in order to gain insights into the, yet poorly known, processes responsible for the shaping of bipolar pPNe.

Methods. We performed high-resolution observations of the H₂O 6_{1,6}-5_{2,3} and ²⁸SiO $v=2, J=1-0$ maser emissions with the Very Long Baseline Array. The absolute position of both emission distributions were recovered using the phase referencing technique, and accurately registered in HST optical images.

Results. Maps of both masers were produced and compared. H₂O maser clumps are found to be distributed in two areas of 20 mas in size spatially displaced by ~60 milli-arcseconds along an axis oriented nearly north-south. SiO masers are tentatively found to be placed between the two H₂O maser emitting regions, probably indicating the position of the Mira component of the system.

Conclusions. The SiO maser emission traces an inner equatorial component with a diameter of 12 AU, probably a disk rotating around the M-type star. Outwards, we detect in the H₂O data a pair of polar caps, separated by 80 AU. We believe that the inner regions of the nebula probably have been altered by the presence of the companion, leading to an equator-to-pole density contrast that may explain the lack of H₂O masers and strong SiO maser emission in the denser, equatorial regions.

Key words. radio lines: stars – masers – technique: interferometric – stars : circumstellar matter – stars : post AGB

1. Introduction

OH 231.8+4.2 (hereafter OH 231.8) is a well studied preplanetary nebula (pPN). The central source is a binary system formed by an M9-10 III Mira variable (i.e. an AGB star) and a A0 main sequence companion, as revealed by optical spectroscopy (see Sánchez Contreras et al. 2004). This remarkable bipolar nebula shows all the signs of post-AGB evolution: fast bipolar outflows with velocities ~200–400 km s⁻¹, shock-excited gas and shock-induced chemistry. The distance of this source, ~ 1500 pc, and the inclination of the bipolar axis with respect to the plane of the sky, ~ 36°, are well known, in particular thanks to measurements of phase lags between the variability of the radiation coming from the two lobes and of the light polarization in them (see Bowers & Morris 1984; Kastner et al. 1992; Shure et al. 1995). The presence of a late-type star in the core of a bipolar post-AGB nebula like OH 231.8 is very unusual since the central stars of pPNe are typically hotter, with spectral types from B to K. PNe and pPNe usually present conspicuous departures from spherical symmetry, including e.g.

multiple lobes and jets. To explain their evolution from spherical AGB envelopes, several models have postulated the presence of dense rings or disks close to the central post-AGB stars (see Soker 2002; Frank & Blackman 2004, e.g.). The accretion of material from them would drive the post-AGB jets by magnetocentrifugal launching, in a similar way as in protostars. The interaction of these jets with the AGB envelope give rise to shocks that shape and accelerate the pPN lobes. Existing observations reveal the presence of central disks in a few pPNe, but their limited spatial resolution cannot unveil the very inner regions of the disks that are relevant for the processes mentioned above.

From mid-infrared MIDI observations of OH 231.8, Matsuura et al. (2006) show the presence of a compact circumstellar region with an inner radius of 40-50 AU (~35 milliarcsec (mas) at 1.3 kpc). An equatorial torus is observed at distances larger than 1 arcsec, however, no trace of rotation is found at this scale and the gas is known to be in expansion, as shown by CO and OH emission data (e.g. Alcolea et al. 2001; Zijlstra et al. 2001).

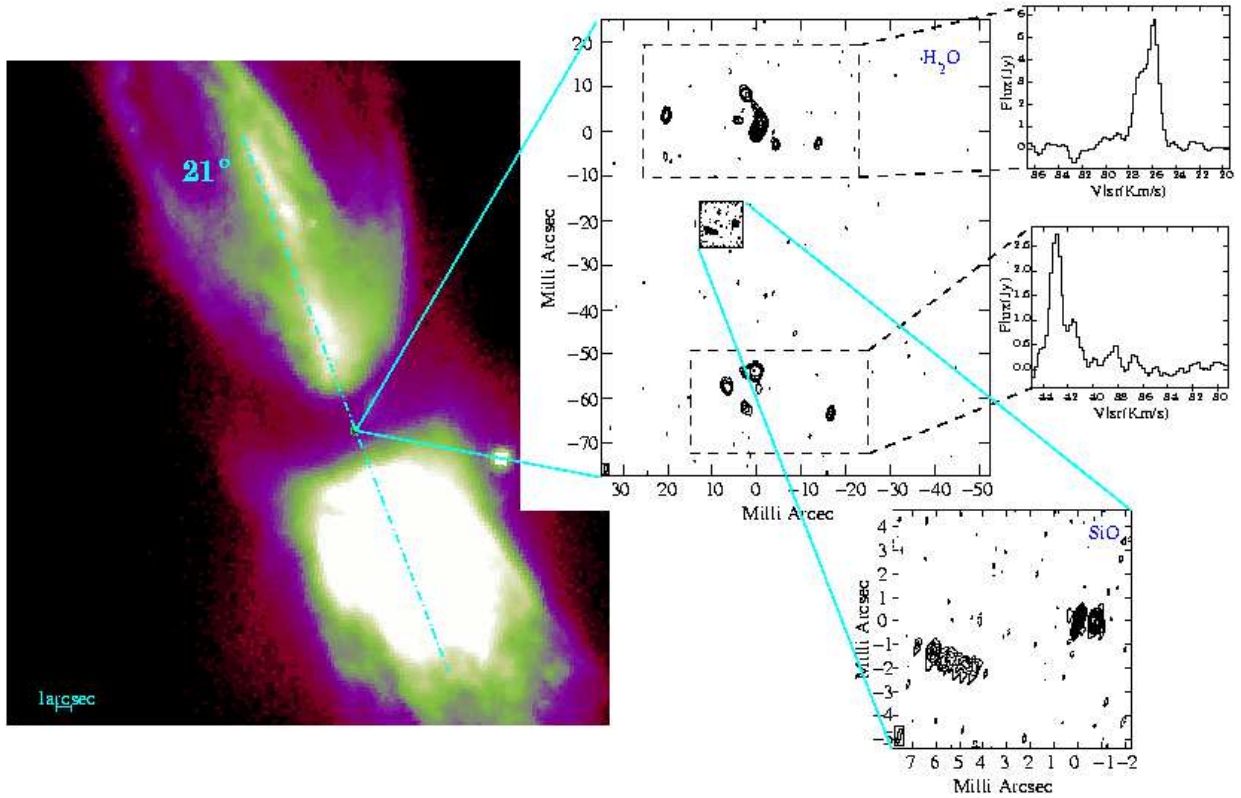


Fig. 1. Total intensity map of the H₂O maser, compared with the *HST* image of the nebula (taken with the WFPC2, filter F791W); accurate astrometry has been performed for the *HST* image and maser maps. The small square map indicates the absolute position of the SiO maser, and the SiO map reproduces the SiO data by Sánchez Contreras et al. (2002). Top right panels show the composed profile of H₂O maser for the two main regions.

Due to the late spectral type ($T_{\text{eff}} \sim 2500$ K) of its AGB central star, OH 231.8 still shows intense SiO masers, contrarily to what happens in the majority of pPNe. NRAO¹ Very Long Baseline Array (VLBA) observations of ²⁸SiO masers in OH 231.8, carried out at 7 mm ($\nu=2$, $J=1-0$) in April 2000 revealed for the first time the structure and kinematics of the close stellar environment in a pPN (Sánchez Contreras et al. 2002). The SiO maser emission arises from several compact, bright spots forming a structure elongated in the direction perpendicular to the symmetry axis of the nebula. Such a distribution is consistent with an equatorial torus with a radius of ~ 6 AU around the central star. A complex velocity gradient was found along the torus, which suggests rotation and infall of material towards the star. Such a distribution is remarkably different from that typically found in maps of AGB stars, where the masers form a roughly spherical ring-like chain of spots resulting from tangential maser amplification in a thin, spherical shell (Desmurs et al. 2000; Cotton et al. 2004).

Water vapor masers are very often observed in AGB envelopes. They occur in regions extending between 30 and 70 AU, therefore, about 5 times larger than the SiO maser shells. Although, in pPNe, water masers are rarely observed, they have been detected in OH231.8. VLA maps of the H₂O emission

by Gómez & Rodríguez (2001) show it to be coincident in position with the SiO masers, but their resolution (about 1 arcsec) was not enough to resolve its structure, as expected. Here, we present VLBA observations of these masers as well as new maps of the SiO maser emission. In both cases we have been able to obtain the absolute position of the spots with great accuracy, and locate them with respect to the other (more extended) components of the nebulae.

2. Observations and astrometry

Using the VLBA, we performed milliarcsecond resolution observations of the H₂O $6_{1,6}-5_{2,3}$ and SiO ($\nu=1$ and $\nu=2$, $J=1-0$) maser emission in the pPN OH 231.8. The H₂O and SiO observations were performed on 24th November 2002 and on 3rd July 2003, respectively. The data were recorded in dual circular polarization with a velocity resolution (i.e. channel width) of ~ 0.2 km s⁻¹ and a total velocity coverage of about 110 km s⁻¹. To be able to measure the relative position of the H₂O and SiO maser spots / clumps part of the observations was made using the phase referencing technique: to ensure the detection of our source, we alternate standard line observations with observations in phase referencing, each observing block lasting 40 minutes. The coordinates are then absolute positions referred to the quasar J0730-11. For the correlation of all the observations, we used the coordinates given by

¹ The National Radio Astronomy Observatory is a facility of the National Science Foundation operated under cooperative agreement by Associated Universities, Inc.

Table 1. Detected H₂O maser components.

| Num | Δ R.A. (mas) | Δ Dec (mas) | V_{lsr} km s ⁻¹ | Peak flux Jy | Width km s ⁻¹ |
|-----------------|------------------------|-----------------------|---------------------------------|-----------------|-----------------------------|
| 1 | 0 | 0 | 25.5 | 12.3 | 2.0 |
| 2 | -0.89 | 2.55 | 27.2 | 5 | 2.0 |
| 3 | 20.31 | 3.72 | 29.1 | 2.5 | 1.4 |
| 4 | 2.38 | 8.35 | 27.8 | 1.8 | 1.9 |
| 5 | -4.25 | -2.82 | 26.6 | 0.7 | 0.9 |
| 6 | -13.86 | -2.62 | 27.4 | 0.56 | 0.6 |
| 7 | 4.16 | 2.46 | 25.4 | 0.4 | 0.4 |
| 8 | 8 | 6 | 20.8 | 0.3 | 0.4 |
| 9 | 21 | -5.0 | 30.3 | 0.2 | 0.3 |
| 10 | 0.33 | -53.90 | 42.9 | 2.9 | 2.3 |
| 11 | -16.68 | -63.36 | 38.5 | 1.5 | 2.4 |
| 12 | 6.57 | -57.48 | 41.9 | 1.3 | 2.3 |
| 13 | 2.55 | -62.06 | 41.6 | 0.85 | 0.9 |
| 14 | 3.03 | -53.84 | 43.1 | 0.59 | 0.8 |
| 15 | 0.1 | -57.60 | 44.4 | 1.3 | 0.6 |
| 16 ^a | -58 | -54 | 40.8 | 0.1 | 0.6 |

^a Outside of the map

Sánchez Contreras et al. (2000), derived from IRAM plateau de Bure observations (R.A._{J2000} = 07^h42^m16^s.93 Dec_{J2000} = -14°42′50″.2).

The data reduction followed the standard scheme for spectral line calibration data in the Astronomical Image Processing System (AIPS). The amplitude was calibrated using the template spectra method. To improve the phase calibration solutions, we extensively mapped all the calibrators, and their brightness distributions were introduced and taken into account in the calibration process.

2.1. Relative position of H₂O and SiO emission

In order to compare the SiO and the H₂O maser emission, the observations were performed using the phase referencing technique. This means that the antennas were rapidly switched between our source (OH231.8) and our calibrator J0730-11 in less time than the phase coherence time of the atmosphere at the given frequency (less than 1 minute for the full switching cycle). Therefore during the data reduction process, we were able to directly apply the phase correction derived from our phase calibrator onto OH231.8. (J0730-11 was well detected at both frequencies with a flux density measured in the resulting maps of 1.44 Jy at 22 GHz, and 1.33 Jy at 43 GHz).

For the water maser observations the phase referencing worked perfectly and the most intense channel of the autocorrelation spectra (the peak lying at 25.5 km s⁻¹ LSR) was easily detected and mapped with a signal-to-noise ratio over 10 σ . The measured absolute position lies at R.A. and Dec offsets Δ (R.A.)=-149 mas and Δ (Dec.)=+166 mas from the correlation position. Therefore, the position measured for our reference H₂O maser spot is R.A._{J2000} = 07^h42^m16^s.91974 Dec_{J2000} = -14°42′50″.0354.

The SiO maser line ($v=2$, $J=1-0$) was weak at the time of the observations, only a few Jy, and the phase referenced map is noisy. The SiO maser profile in our data is composed

of three peaks, at about 26, 32 and 40 km s⁻¹ LSR, similar to those observed in other epochs in the source, see e.g. Sánchez Contreras et al. (2000, 2002). We were able to map the emission in the most intense channel, the one lying close to 27 km s⁻¹ LSR, and identified a feature with a flux of 72.55 mJy i.e. at a level of 4.4 σ detection. This tentative detection for the SiO maser emission give us an absolute position at offsets Δ (R.A.)=-145 mas and Δ (Dec.)=+145 mas with respect to the correlation position. The absolute coordinates of our reference SiO feature would be: R.A.= 07^h42^m16^s.91994 Dec= -14°42′50″.0574. This would place the SiO maser emission nearly in the middle of the two groups of water maser spots (see Fig. 1). The SiO map shown in Fig. 1 is that obtained by Sánchez Contreras et al. (2002), aligned under the assumption that the position derived by us coincides with the centroid of their spot distribution. Because of the small size of the SiO maser distribution, the uncertainty of this alignment is in any case very small, less than about 3 mas.

In order to locate the SiO and H₂O maser spots in the HST image of the nebula, we improved the astrometry of the HST images published by some of us (Bujarrabal et al. 2002). In that paper, the registering of the images was done with IRAF using the “STSDAS” task “metric” by comparing the positions of 28 stars in the FWPC2 chips listed in the Guide Star Catalog 2.2 with those retrieved by the task. We concluded that, after corrections, the positions of the plates were accurate up to 0.2 arcsec. Since then, the Second U.S. Naval Observatory CCD Astrograph Catalog (Zacharias et al. 2004) has been released. We have 9 stars in the 4 FWPC2 chips listed in this catalog with position errors of about 0.02 arcsec. or less. We have compared these nominal positions with those derived with the task “metric” obtaining mean errors (measured – nominal) of -0′.81 to the east (-0.056 sec. of time in R.A.) and -0′.43 in Dec, with rms of 0′.12 and 0′.054 respectively (fully consistent with the values of -0′.6 \pm 0′.2 and -0′.5 \pm 0′.2 obtained by Bujarrabal et al. 2002). Using these corrections we have plotted the location of both maser emissions on the HST plate shown in Fig. 1.

3. Results and discussion

In Table 1 we summarise our H₂O observational results. Column 2 and 3 give the offset in mas of each maser spot respectively to the reference maser spot. This reference maser was used to derive the fringe rate corrections, and is the one for which we measured the absolute position with respect to the quasar. The three last columns give the values obtained from Gauss fit of each maser spot, central velocity, peak flux intensities, and the full linewidth at half peak intensity.

The H₂O maser integrated flux map is shown in Fig. 1. The restored clean beam has a full width at half maximum of about \sim 1.5 x 0.75 mas, and is oriented with a position angle of PA = -5°. Maser emission has been searched for a large area of up to 900 mas. Maps have been cleaned down to a noise level of 30 mJy/beam. Maser emission arises from several compact spots distributed in mainly two areas, separated by about 60 mas, in approximately the north-south direction, corresponding to the two spectral features appearing on the auto

and cross correlation spectra (note that we also found an isolated maser spot at a few tenths of mas to the west). The northern area correspond to the blue-shifted emission and the southern to the red-shifted one. Our SiO observations indicate that the SiO masers arise from a region placed approximately in the middle of both H₂O maser-emitting areas (see Fig. 1), probably pinpointing the location of the central Mira component of the central stellar system.

The size of the water maser regions around AGB stars varies between $\sim 5 \cdot 10^{14}$ and $2 \cdot 10^{15}$ cm (e.g. Colomer et al. 2000; Bains et al. 2003), occupying the circumstellar region in which the expansion velocity is already high but probably has not yet reached its final value (around 8–10 km s⁻¹). The distribution of the maser spots in some objects (IRC +60169, U Her, IK Tau, RT Vir, ...), is rounded and consistent with the maser emission arising in a thick expanding shell. In other objects, the distribution of the maser spot is more chaotic.

It is thought that, at a distance of a few 10^{14} cm from the AGB star, the temperature (500 – 1000 K) and densities ($5 \cdot 10^7 - 10^9$ cm⁻³, for standard mass-loss rates between $\sim 10^{-6}$ and $10^{-5} M_{\odot}$ yr⁻¹) are adequate to produce strong H₂O maser emission (see model predictions by e.g. Cooke & Elitzur 1985). Water abundances in these layers are still high, more or less equal to those given by thermal equilibrium.

As we have seen, the size of the total emitting region in OH 231.8, $\sim 10^{15}$ cm, is very compatible with that in standard red giants. Also the spot relative velocity, requiring a deprojected expansion velocity of 10 - 15 km s⁻¹ (for an axis inclination of about 36° with respect to the plane of the sky, Sect. 1), is compatible with the usual velocities found in AGB stars (e.g. Loup et al. 1993; Te Lintel Hekkert et al. 1989). However, we note that the total velocity dispersion in our data (~ 20 km s⁻¹) is larger than those found in the majority of H₂O profiles from AGB stars (see e.g. Engels & Lewis 1996; Engels 2002; Colomer et al. 2000; Bains et al. 2003).

Therefore, from the point of view of the pumping conditions and kinematics, the H₂O emission in our object comes from a region that we can assume to be typical of water masers in AGB stars. No special phenomena (shocks, photo induced chemistry, ...) are then necessarily required to explain our observations, just the usual physical and chemical conditions in the envelope of a O-rich AGB star.

The bipolar spatial distribution of H₂O masers in OH 231.8 is, however, peculiar. Instead of a circular distribution around the central star, we find two spot sets. The fact that the SiO maser emission comes from a region in the middle of the H₂O spot areas confirms that they are placed at both sides of the star, along the axis of the nebula. This distribution strongly suggests that the equatorial regions of the inner circumstellar envelope of OH 231.8 have been strongly modified, probably by the presence of a companion, and are now not able to harbor water vapor masers. Running simple modeling of water maser excitation (see Soria-Ruiz et al. 2004), it appears that water masers can be easily quenched: a modification by a factor of 2 of the radius of the emission (this corresponds to a factor 4 in density) produces intensity drop of the maser by one order of magnitude.

Based on its broad OH maser emission profile, OH231.8 has been suggested to be a "water-fountain" cousin (e.g. Likkell et al. 1992). "Water-fountain" sources are a special class of rare post-AGB stars with very high velocity outflows traced by OH or H₂O masers or both. So far there are only four objects in this group, namely: IRAS 16342-3814, IRAS 19134+2131, W43A (e.g. Likkell et al. 1992), and the most recently discovered OH 12.8-0.9 (Boboltz & Marvel 2005). The expansion velocities of the outflows implied by the H₂O maser emission in these objects (except for OH 12.8 - see below), $V_{\text{exp}} = 100 - 300$ km s⁻¹, are one order of magnitude larger than the typical shell expansion velocity of mass-losing evolved stars (see above). Another characteristic of water fountain sources is that the expansion velocity derived from H₂O is higher than that deduced from the OH maser emission. This implies that the location of the masers in these objects deviates from the prototypical maser stratification in AGB envelopes, where the SiO, H₂O, and OH masers arise in different shell layers located at progressively further distances from the star, expanding also at progressively higher velocities. As revealed by recent high-angular resolution observations, the spatial structure of the H₂O masers in water-fountain sources is indeed peculiar: the masers are occur in collimated winds or jets, aligned with the symmetry axis of the nebulae (e.g. Imai et al. 2004; Boboltz & Marvel 2005). These maser spots are located at distances that range between 870 AU and 600 AU from the central star, i.e. much farther away than H₂O masers in OH/IR stars (typically at 40 - 70 AU) and therefore, shock-compression and heating is required to explain the fast maser spots at these distances: the maser emission would be located in an area of shocked gas, in the region where the post-AGB jets interact with the fossil AGB envelope.

Although the nebular geometry model (equatorial disk + polar stream) proposed to explain water-fountain sources probably applies to OH231.8 to some extent, the H₂O maser emission in OH231.8 is remarkably different from that found in water-fountain objects (see above). A few other pPNe show H₂O emission with low-velocity spots, more similar to that observed in our source (de Gregorio-Monsalvo et al. 2004). Although the interpretation of the origin of the H₂O emission in them is not straightforward, it seems to come from nebular regions that have not been accelerated during the post-AGB evolution. In particular, the expansion velocity of the H₂O masers is very low compared to pPN bipolar jets. Moreover, the H₂O emission is not as well collimated as in water-fountains. As a consequence, shocks effects (expected to be responsible for the pPNe bipolar outflows) are not required to explain the H₂O maser emission in OH231.8, which is observed at only ~ 40 AU from the central star, as in normal AGB envelopes, and expanding at low velocity, lower than that of the OH maser spots.

We cannot rule out that the H₂O maser spots of OH231.8 are placed at the base of a bipolar outflow, whose very fast, extended components are detected in scattered light and CO line emission. In this case, the masers would lie there because a bipolar ejection of material has yielded two opposite condensations with suitable conditions to form H₂O masers. But, as discussed above, the properties of water vapor masers in our source are very different from those of maser associated with

bipolar outflows in pPNe. In fact, they resemble those of H₂O masers associated with AGB stars. We also note that if the H₂O masers are tracing a bipolar outflow, this would be expected to be centered around the compact companion of the binary system, which is most likely to power the jets in this case (e.g. Sánchez Contreras et al. 2004), and not around the mass-losing star, i.e. the Mira, as we observe.

In summary, in view of their spatial distribution and kinematics, the maser spots in OH 231.8 seem to be the result of a pumping process very similar to that at work in AGB circumstellar envelopes, and under similar physical and chemical conditions. But they take place in an envelope that has been seriously altered, probably due to the presence of a companion, in such a way that only (unshocked) polar regions of the envelope keep favorable conditions for H₂O maser pumping. The fact that the SiO maser region is much smaller than the H₂O region and perpendicular to its distribution, probably indicates that gravitational/tidal forces due to the companion strongly affect these inner circumstellar shells, supporting our conclusion on its effects on the H₂O emitting region.

References

- Alcolea, J., Bujarrabal, V., Sánchez Contreras, C., Neri, R., & Zweigle, J. 2001, *A&A*, 373, 932
- Bains, I., Cohen, R. J., Louridas, A., et al. 2003, *MNRAS*, 342, 8
- Boboltz, D. A. & Marvel, K. B. 2005, *ApJ*, 627, L45
- Bowers, P. F. & Morris, M. 1984, *ApJ*, 276, 646
- Bujarrabal, V., Alcolea, J., Sánchez Contreras, C., & Sahai, R. 2002, *A&A*, 389, 271
- Colomer, F., Reid, M. J., Menten, K. M., & Bujarrabal, V. 2000, *A&A*, 355, 979
- Cooke, B. & Elitzur, M. 1985, *ApJ*, 295, 175
- Cotton, W. D., Mennesson, B., Diamond, P. J., et al. 2004, *A&A*, 414, 275
- de Gregorio-Monsalvo, I., Gómez, Y., Anglada, G., et al. 2004, *ApJ*, 601, 921
- Desmurs, J. F., Bujarrabal, V., Colomer, F., & Alcolea, J. 2000, *A&A*, 360, 189
- Engels, D. 2002, *A&A*, 388, 252
- Engels, D. & Lewis, B. M. 1996, *A&AS*, 116, 117
- Frank, A. & Blackman, E. G. 2004, *ApJ*, 614, 737
- Gómez, Y. & Rodríguez, L. F. 2001, *ApJ*, 557, L109
- Imai, H., Morris, M., Sahai, R., Hachisuka, K., & Azzollini F., J. R. 2004, *A&A*, 420, 265
- Kastner, J. H., Weintraub, D. A., Zuckerman, B., et al. 1992, *ApJ*, 398, 552
- Likkel, L., Morris, M., & Maddalena, R. J. 1992, *A&A*, 256, 581
- Loup, C., Forveille, T., Omont, A., & Paul, J. F. 1993, *A&AS*, 99, 291
- Matsuura, M., Chesneau, O., Zijlstra, A. A., et al. 2006, *ApJ*, 646, L123
- Sánchez Contreras, C., Bujarrabal, V., Neri, R., & Alcolea, J. 2000, *A&A*, 357, 651
- Sánchez Contreras, C., Desmurs, J. F., Bujarrabal, V., Alcolea, J., & Colomer, F. 2002, *A&A*, 385, L1
- Sánchez Contreras, C., Gil de Paz, A., & Sahai, R. 2004, *ApJ*, 616, 519
- Shure, M., Sellgren, K., Jones, T. J., & Klebe, D. 1995, *AJ*, 109, 721
- Soker, N. 2002, *ApJ*, 568, 726
- Soria-Ruiz, R., Alcolea, J., Colomer, F., et al. 2004, *A&A*, 426, 131
- Te Lintel Hekkert, P., Versteeg-Hensel, H. A., Habing, H. J., & Wiertz, M. 1989, *A&AS*, 78, 399
- Zacharias, N., Urban, S. E., Zacharias, M. I., et al. 2004, *AJ*, 127, 3043
- Zijlstra, A. A., Chapman, J. M., te Lintel Hekkert, P., et al. 2001, *MNRAS*, 322, 280